Research article

Spreading depolarization evoked by endothelin-1 is inhibited by octanol but not by carbenoxolone

Gabor C. Petzold [a,b], Jens P. Dreier [c,d,e,f,g,*,1]

[a] German Center for Neurodegenerative Diseases (DZNE), Venusberg-Campus 1, 53127 Bonn, Germany
[b] Division of Vascular Neurology, Department of Neurology, University Hospital Bonn, Venusberg-Campus 1, 53127 Bonn, Germany
[c] Center for Stroke Research Berlin, Charité – Universitätsmedizin Berlin, Corporate Member of Freie Universität Berlin, Humboldt-Universität zu Berlin, and Berlin Institute of Health, Berlin, Germany
[d] Department of Experimental Neurology, Charité – Universitätsmedizin Berlin, Corporate Member of Freie Universität Berlin, Humboldt-Universität zu Berlin, and Berlin Institute of Health, Berlin, Germany
[e] Department of Neurology, Charité – Universitätsmedizin Berlin, Corporate Member of Freie Universität Berlin, Humboldt-Universität zu Berlin, and Berlin Institute of Health, Berlin, Germany
[f] Bernstein Center for Computational Neuroscience Berlin, Berlin, Germany
[g] Einstein Center for Neurosciences Berlin, Berlin, Germany

ARTICLE INFO

ABSTRACT

Spreading depolarization (SD) has been implicated in the pathogenesis of delayed cerebral ischemia (DCI) after subarachnoid hemorrhage. Endothelin-1 (ET-1) is a powerful trigger of SD and may be involved in DCI. The SD-causing mechanism is assumed to result from ET-1-induced microarterial spasm and ischemia. However, ET-1 is also a potent, astrocyte-specific gap junction (GJ) inhibitor. There are two competing hypotheses on the role of astrocytic GJs in SD. One postulates that they mediate SDs, since long-chain alcohols such as octanol inhibit GJs and inhibit SD at high concentrations. The other postulates that astrocytic GJs protect against SD and that their inhibition increases susceptibility to SD and SD velocity. Here, we found in rats that brain topical application of carbenoxolone, a more specific GJ inhibitor, failed to inhibit ET-1-induced SDs in vivo, whereas octanol, a less specific GJ inhibitor, partially blocked them at high concentrations. These results suggest that GJs are not required for initiation or propagation of ET-1-induced SDs, and that octanol inhibits SDs by effects unrelated to GJs. The results do not exclude that the specific inhibition of astrocytic GJs by ET-1 contributes to the generation of SDs, which should be further investigated in future studies.

© 2020 International Hemorrhagic Stroke Association. Publishing services by Elsevier B.V. on behalf of KeAi Communications Co. Ltd. This is an open access article under the CC BY-NC-ND license (http://creativecommons.org/licenses/by-nc-nd/4.0/).

1. Introduction

Delayed cerebral ischemia (DCI) contributes to the morbidity and mortality following aneurysmal subarachnoid hemorrhage (aSAH).[1,2] In autopsy and imaging studies, cortical ischemic lesions are the predominant pattern of parenchymal damage both in patients with aSAH[3–7] and in the non-human primate model of SAH.[8] Ischemia forces neurons to fall into the state of cytotoxic edema with a certain delay when the ATP reserve supplying the Na,K-ATPases is depleted and the Na,K-ATPases are no longer able to maintain the ion gradients across the neuronal cell membrane.

This is visualized as a diffusion restriction using diffusion-weighted magnetic resonance imaging.[9,10] The term spreading depolarization (SD) describes the mechanism of sustained neuronal mass depolarization, near-complete collapse of the transmembrane ion gradients, abrupt inflow of water into neurons, trapped in beads of their dendrites, that causes and maintains the cytotoxic edema and the diffusion restriction in the brain's gray matter.[10–18] Thus, SD marks the onset of the toxic changes that eventually lead to cell death. However, SD is not a marker of cell death per se, since the toxic changes are reversible – up to a point – with restoration of the blood flow and energy supply. The term SD continuum describes the spectrum from terminal SD in severely ischemic tissue to transient SDs with negative direct current (DC) shifts of intermediate to short duration in less ischemic or normal tissue.[19,20] Consistent with the fundamental role of SD as electrophysiological correlate of acute neuronal injury in the brain's gray

* Corresponding author at: Center for Stroke Research, Campus Charité Mitte, Charité – Universitätsmedizin Berlin, Charitéplatz 1, 10117 Berlin, Germany.
E-mail address: jens.dreier@charite.de (J.P. Dreier).
[1] orcid.org/0000-0001-7459-2828.

matter, SDs have been abundantly found in aSAH patients during both the early and delayed time period[21–27] as well as in patients with ischemic stroke secondary to proximal artery occlusion,[28–30] traumatic brain injury (TBI)[31,32] and spontaneous intracerebral hemorrhage,[33] and in animal models of SAH,[24,34–37] ischemic stroke[38–41] and TBI.[42,43]

After the onset of severe ischemia, SD usually begins to spread from one or more spots in the ischemic core with a delay of at least one minute.[23,44] This seems to be the minimum time required for the ATP concentration to drop below the critical threshold. However, a typical characteristic of DCI is its slow, gradual development after aSAH. Under this condition, considerably more time elapses before the first SD occurs. An animal model that is particularly well suited to investigate the constellation of a gradually developing and milder form of ischemia in the brain cortex is the model of brain-topical application of endothelin-1 (ET-1),[45] although it should be noted that ET-1 alone is not sufficient to explain DCI. Thus, ET receptor antagonists robustly inhibited the angiographic arterial spasm after aSAH in clinical trials, but no effect was observed on new cerebral infarctions or case-fatality.[46,47]

In animal experiments, ET-1 is indeed the most potent chemical compound currently known to induce SDs.[45] Even topical application of a concentration of 10 nM to the cerebral cortex can be sufficient to induce SD in vivo.[48] At this low concentration, ET-1 often induces a single mildy prolonged SD and at increasing concentrations, a cluster of prolonged SDs superimposed on a shallow negative ultraslow potential.[45] The pattern of a typical terminal SD, where the SD changes into a negative ultraslow potential with high amplitude, can only be seen at even higher concentrations.[49] SD can also be triggered by many other factors such as, for example, an elevated extracellular K^+ concentration ($[K^+]_o$), Na^+ channel openers or Na,K-ATPase inhibitors that do not mediate SD via ischemia but direct targets on neurons or astrocytes.[50–55] Yet, several arguments suggest that ET-1-induced SDs result from ET-1-induced vasoconstriction and ischemia. First, the direct imaging of pial arterioles showed significant narrowing, especially of vessels with medium and small diameters before ET-1-induced SDs.[49] This was accompanied by a significant decrease in regional cerebral blood flow (CBF) and tissue partial pressure of oxygen.[45,56] Second, ET-1-induced SDs are preceded by ion changes such as a mild increase of the extracellular K^+ concentration ($[K^+]_o$) and a mild acidosis that typically occur in ischemia but are not observed prior to SDs migrating through healthy, adequately perfused tissue.[45,49] Third, the receptor profile indicated ischemia as the cause of ET-1-induced SDs, as the ET_A receptor antagonist BQ-123 was sufficient to prevent the SDs.[48] Fourth, the development of selective neuronal necrosis after ET-1-induced SDs supported the hypothesis that the SDs resulted from ischemia, since necrosis does not usually occur when SDs migrate through metabolically intact tissue.[49,57,58] Finally, ET-1-induced SDs, in contrast to SDs induced by agents acting on non-vascular targets, did not occur in neocortical slices.[45] This supports the hypothesis that ET-1 induces SD by vasoconstriction and ischemia because there is no intact circulation in brain slices. The supply of glucose and oxygen to brain slices takes place via the perfused medium and the gas–liquid interface instead of via the circulation.

However, ET-1 is not only a vasoconstrictor but also a highly potent, astrocyte-specific gap junction (GJ) inhibitor.[59–62] This is interesting because previous studies have suggested that astrocytic GJs mediate the spread of SDs.[63,64] This hypothesis has been based on observations that neurons in cell culture can respond to interastrocytic Ca^{2+} waves with large increases in their concentration of cytosolic Ca^{2+}, that an interastrocytic Ca^{2+} wave accompanies SD, and that GJ inhibitors such as heptanol and octanol inhibit SDs.[63,65,66] However, subsequent studies provided evidence that SD is primarily a neuronal rather than an astrocytic phe-

nomenon.[67–69] For example, the interastrocytic Ca^{2+} wave that accompanies SD was attenuated by the specific GJ blocker carbenoxolone at 100 μM without affecting SD.[70] To address the open question whether the effects of octanol on SD specifically arise from a blockade of astrocytic GJs, we here tested the effects of octanol and the more specific GJ inhibitor carbenoxolone on ET-1-induced SDs. Our premise was that since astrocytic GJs are already blocked by ET-1, octanol specifically in this model unlike in other models should not inhibit SDs.[63,71–73]

2. Materials and methods

The reporting of animal experiments complies with the Animal Research: Reporting of In Vivo Experiments (ARRIVE) Guidelines. All animal experiments were authorized by the animal welfare authorities in Berlin, Germany: Berlin State Office for Health and Social Affairs (LAGeSo), G0346/98, and all experimental procedures were conducted in accordance with the Charité Animal Welfare Guidelines. The animals were housed in groups (2–4 animals per cage) under a 12 h light/dark cycle with food and tap water available ad libitum.

2.1. Animal preparation and experimental set-up

Twenty male Wistar rats (250–400 g; Charles River Laboratories, Wilmington, MA, USA) were anesthetized with 100 mg/kg thiopental sodium intraperitoneally (Trapanal, BYK Pharmaceuticals and artificially ventilated (Effenberger Rodent Respirator; Effenberger Med.-Techn. Gerätebau, Pfaffing/Attel, Germany) to maintain an arterial partial pressure of CO_2 (pCO_2) between 35 and 45 mmHg, an arterial pO_2 between 90 and 130 mmHg and an arterial pH between 7.35 and 7.45. The right femoral artery and vein were cannulated and saline solution was continuously infused (1 ml/h). Systemic arterial pressure (RFT Biomonitor, Zwönitz, Germany) and expiratory pCO_2 (Heyer CO_2 Monitor EGM I, Bad Ems, Germany) were continuously monitored. Arterial pO_2, pCO_2, and pH were serially measured using a Compact 1 Blood Gas Analyzer (AVL Medizintechnik GmbH, Bad Homburg, Germany). Body temperature was maintained at 37.5 ± 0.5 °C using a heating pad (Temperature Control FHC, Bowdoinham, ME, USA). The level of anesthesia was assessed by testing motor responses and changes in blood pressure to foot-pinching. If necessary, additional doses of thiopental (25 mg/kg body weight) were applied.

For all experiments, two separate closed cranial windows (diameter, ~4 mm each) were implanted over the ipsilateral caudal and rostral cortex following craniotomy and dura mater removal as described.[52] The distance between both windows was 5 mm. CBF was monitored by two laser-Doppler probes (Perimed, Järfälla, Sweden), with one probe placed over each window. The subarachnoid DC-potential at each window was measured by Ag/AgCl-electrodes as reported in previous studies in which this recording technique was validated using intracortical microelectrodes.[49,74,75] Blood pressure, CBF and DC-potential were continuously recorded using a PC-coupled chart recorder (DASH-IV).

In group 1 (n = 8), each experiment started with superfusion of the cortex in each window with aerated physiological artificial cerebrospinal fluid (ACSF; in mM: 152 NaCl/3 KCl/1.5 $CaCl_2$/24.5 $NaHCO_3$/1.2 $MgCl_2$/3.7 glucose/6.7 urea) through separate syringe pumps, and baseline CBF was measured for 60 min. Subsequently, ET-1 solubilized in ACSF at increasing concentrations was continuously applied to one window (100 nM for 60 min, followed by 1 μM for 60 min) until an SD was detected in this (ET-1perfused) window that propagated into cortex underlying the other (ACSF-perfused) window.

In group 2 (n = 6), the experiments started with superfusion of the cortex in each window with aerated physiological ACSF as described above. Subsequently, carbenoxolone (1 mM) in ACSF was applied to one window for 60 min, followed by increasing concentrations of ET-1 (as described above) together with carbenoxolone. If no SD had occurred after 60 min of carbenoxolone and 1 μM ET-1, ET-1 was applied alone for 60 min at 1 μM to elicit an SD as a positive control.

Experiments in group 3 (n = 6) were conducted exactly as in group 2, with the difference that octanol (2 mM) was applied instead of carbenoxolone. CBF and DC-potential were continuously monitored in all groups as described above.

2.2. Pharmacology

All reagents were purchased from Sigma-Aldrich and diluted in ACSF unless otherwise stated. The concentrations of ET-1 necessary to trigger SD were derived from our own previous studies.[45,57] The concentration of carbenoxolone (1 mM) was inferred from studies that showed that similar or even lower concentrations of carbenoxolone inhibited electrographic seizures in vivo.[76,77] Octanol was prepared as a 1 M stock solution in ethanol and diluted in ACSF to 2 mM, which is the usual concentration for topical administration in vivo.[78] Ethanol at the final concentration used in this study (29 mM) has no effect on SD.[72]

2.3. Statistical analysis

Data were analyzed by comparing CBF changes in relation to baseline (=100 %) and absolute DC-potential changes (amplitude and duration at half-maximal amplitude). Electrophysiological and CBF changes between the two windows were compared using the paired t-test. The ET-1 concentrations necessary to generate the first SD, i.e. the SD threshold, were compared using Fisher's Exact Test. The propagating nature of the recorded electrophysiological events was verified by the typical DC-potential and CBF changes associated with SD in the window perfused with ET-1, followed by similar changes in the separate ACSF-perfused window. SD propagation velocity was determined by dividing the distance between both electrodes by the temporal lag of the beginning of the negative DC-potential deflection in the caudal and the cranial window. $P < 0.05$ was accepted as statistically significant. All data in the text and figures are given as mean values ± standard deviation.

3. Results

The systemic variables remained within physiological limits throughout the experiments (Table 1).

3.1. Characteristics of SD generated by ET-1 in vivo

We implanted two cranial windows over the ipsilateral hemisphere. ET-1 was applied at increasing concentrations (100 nM and 1 μM for 60 min each) at one window to generate SD, while physiological ACSF was continuously applied to the other window (n = 8). CBF and DC-potential changes were recorded at both windows to monitor SD. The typical pattern of SD at the ET-1 window in comparison to SD at the control window is illustrated in Fig. 1. In 5 animals, SD occurred at a concentration of ET-1 of 100 nM and subsequently also occurred at a concentration of ET-1 of 1 μM (Fig. 2A). In the remaining 3 animals, SD only occurred at an ET-1 concentration of 1 μM (Fig. 2A). Preceding SD, a gradual significant decrease of baseline CBF was observed in response to ET-1, compared to constant CBF levels at the window perfused with

physiological ACSF (Fig. 2B). SD at the window superfused with ET-1 was characterized by a negative DC-shift of −4.5 ± 1.5 mV that lasted for 81 ± 21 s. In comparison, SD at the control window consisted of a negative DC-shift of −4.3 ± 1.8 mV lasting for 54 ± 11 s. Thus, the DC shifts observed at the ET-1 window were significantly longer (Fig. 2C).

CBF changes typical of SD occurred at both windows: a mild variable hypoperfusion, followed by transient hyperemia and mild long-lasting oligemia.[52] The initial hypoperfusion was significantly more pronounced at the ET-1 window compared to control (Fig. 2D), while the duration was similar (14 ± 8 s vs. 16 ± 9 s, paired t-test). The subsequent transient hyperemia was significantly smaller at the ET-1 window (Fig. 2D). The levels of the oligemic phase were similar at both windows (Fig. 2D). The propagation velocity of the first SD between the windows was 3.9 ± 0.2 mm/min.

3.2. Carbenoxolone does not inhibit ET-1-induced SD

We next tested the sensitivity of SD generated by ET-1 to the relatively specific GJ blocker carbenoxolone (n = 6). Carbenoxolone (1 mM) was applied to one window for 60 min, followed by co-application of carbenoxolone with ET-1 at increasing concentrations.

SD occurred at 100 nM ET-1 in 3 animals and at 1 μM in the remainder (Fig. 2E). Thus, the threshold for the generation of SD was similar to animals receiving ET-1 without carbenoxolone (p > 0.05, Fisher's Exact Test). CBF slightly but significantly increased during application of carbenoxolone alone compared to the control window (Fig. 2F), and the subsequent addition of ET-1 at increasing concentrations led to a significant reduction of CBF compared to levels in the control window (Fig. 2F; CBF before SD at 100 nM ET-1: 81 ± 11%; CBF before SD at 1 μM ET-1: 75 ± 4%). The DC-potential shift at the ET-1 window lasted significantly longer than at the control window (Fig. 2G). SD propagated at a velocity of 3.7 ± 0.5 mm/min. The CBF changes associated with SD were again characterized by a significantly more pronounced hypoperfusion and smaller hyperemia compared to control (Fig. 2H), while the oligemia was similar (Fig. 2H). Hence, carbenoxolone did not change the electrophysiological and neurovascular properties of SD, and the threshold of SD remained unchanged by carbenoxolone.

3.3. Octanol increases the threshold of ET-1-induced SD

In the third group, we tested the effect of the less specific GJ inhibitor octanol on SD (n = 6). Superfusion with octanol alone was started one hour before ET-1 was added. At 100 nM, no animal generated SD in the presence of octanol (Fig. 2I). At 1 μM, 3 animals generated SD (Fig. 2I). In those animals that did not generate SD, 1 μM ET-1 was topically applied for additional 60 min without octanol. In this period, SD occurred in all animals (Fig. 2I). Thus, octanol shifted the threshold concentration of ET-1 to induce SD to a significantly higher range (p < 0.05, Fisher's Exact Test). SD propagation velocity was 4.1 ± 1.0 mm/min. CBF at the window superfused with octanol alone showed a nonsignificant increase compared to the control window (Fig. 2J). ET-1 at 100 nM together with octanol led to a significant CBF decrease (Fig. 2J), and CBF declined further after ET-1 was increased to 1 μM (Fig. 2J). Similar to the other groups, SD in the ET-1 window was characterized by a more pronounced hypoperfusion, smaller hyperemia and longer DC-potential shift compared to control (Fig. 2K-L).

Table 1
Physiological variables.

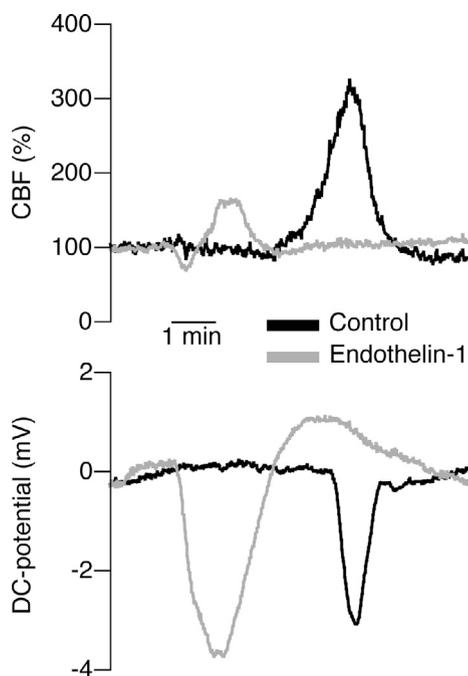|	Mean arterial blood pressure (mm Hg)	PaCO₂ (mm Hg)	PaO₂ (mm Hg)	pH
ET-1	109 ± 11	38.4 ± 5.2	113 ± 6	7.36 ± 0.04
ET-1 + carbenoxolone	104 ± 10	36.9 ± 4.8	110 ± 8	7.35 ± 0.04
ET-1 + octanol	102 ± 16	37.2 ± 4.1	109 ± 8	7.37 ± 0.05

Fig. 1. SD in normal and ET-1-treated cortex. Two cranial windows were implanted over the ipsilateral hemisphere. ET-1 (100 nM) was applied to one window (grey traces), while the second window was perfused with physiological ACSF (black traces). CBF and DC-potential were measured at both windows. ET-1 triggered SD at the first window, characterized by a transient negative deflection of the DC-potential. SD was accompanied by a triphasic CBF change, consisting of an initial hypoperfusion, followed by a transient hyperemia and mild oligemia. Compared to control conditions, SD in the ET-1 window was characterized by a longer deflection of the DC-potential, larger initial hypoperfusion and smaller transient hyperemia. The temporal delay between the two events indicates the slowly propagating nature of SD.

4. Discussion

In the present study, SD evoked by ET-1 was not affected by the GJ blocker carbenoxolone, but partially inhibited by octanol. The failure of carbenoxolone argues against a role for GJs as mediators of SD triggered by ET-1 and further supports the notion that the inhibiting effect of high concentrations of octanol on SD is not related to the inhibition of GJs.

The molecular pathways underlying the generation and propagation of SD have not yet been elucidated. Different hypotheses have been posited according to which GJs play a role in the SD wave. Some of them contradict each other. First, a transcellular pathway via neuronal GJs between pyramidal cells has been suggested in which prodromal neuronal synchronization would occur ahead of the advancing wave front of DC-potential and ionic changes during SD.[79,80] Thus, fast electrical activity, i.e. small rhythmic sawtooth wavelets followed by a shower of population spikes, has been recorded in the front of an approaching SD wave, several seconds before the onset of the DC negativity and extracellular rise in [K⁺]ₒ. This fast activity was synchronized over considerable distances in the tissue and occurred in phase in dendrites and somata in contrast to synaptically transmitted population

spikes. Blocking synaptic transmission did not abolish this prodromal activity. Therefore, it was proposed that the prodromal activity could result from the opening of neuronal GJs.[79] How exactly this would lead to the propagation of the almost complete collapse of the ion gradients and the sustained neuronal depolarization remained open, though. An argument hold against this hypothesis is that the GJ-mediated coupling between pyramidal cells seems to disappear at the end of the second postnatal week,[81,82] and hence neuronal GJs only remain detectable between interneurons.[83–85] In fact, the susceptibility of the brain to SD develops in exactly the opposite way to the development of GJs between pyramidal cells. Thus, typical neonatal brains do not seem to support SD.[86] SD in response to oxygen-glucose deprivation is then observed at postnatal day 5 in rats.[87] Milder stimuli of SD may fail until postnatal day 10 and continue to fail occasionally up to day 20.[88] Subsequently, the susceptibility of the tissue to SD rapidly reaches its peak between days 16 to 30 and slowly decreases again thereafter.[89–91] Yet, it is actually disputed whether all GJs between pyramidal cells disappear during postnatal development. Some authors argue that the typical neuronal GJs based on connexin 36 could be replaced by GJs based on connexin 45.[92] However, another argument against a causative role of neuronal GJs for SD propagation is that carbenoxolone, a potent blocker of astrocytic and neuronal GJs,[77,93–95] did not inhibit SD evoked by a microdrop of KCl in brain slices.[71] In the present study, in agreement with these findings, we found that carbenoxolone did not affect ET-1-induced SDs *in vivo*. We likely achieved sufficient activity of carbenoxolone in the cortex, since similar or lower concentrations are sufficient to block electrographic epileptic seizures.[76,77] Moreover, carbenoxolone possesses low-grade intrinsic vasorelaxant properties,[96] and we found a small but significant increase of CBF in response to carbenoxolone. Given that laser-Doppler flowmetry measures CBF at a depth of ~250–300 μm,[97] this indicates significant diffusion into the tissue. Of note, the failure of carbenoxolone to inhibit SD is not necessarily an argument against GJ-mediated prodromal synchronization ahead of the SD wave. In the context of the prodromal synchronization, neuronal GJs between interneurons have not yet been investigated to our knowledge. We believe that they should also be included in these considerations. This applies in particular because recent work on familial hemiplegic migraine type 3, one of the Mendelian model diseases of SDs, suggests that the role of interneurons in the SD process has so far been underestimated.[98,99]

Another theory has posited that SD propagation is mediated by astrocytic GJs.[63,65] However, it has been found independently using intracellular Ca²⁺ measurements that neurons lead and astrocytes follow in the wave front of SD.[68,69] Moreover, Theis and colleagues observed that increases rather than decreases of SD velocity and susceptibility occur in genetically modified mice, in which astrocyte-directed inactivation of connexin 43 decreased astrocytic gap-junctional communication.[100] Another argument is that ET-1, a strong, astrocyte-specific GJ inhibitor[59–62] does not inhibit SDs, but potently triggers them *in vivo* as shown in the present and previous studies.[45,49,57] Based on the findings of Theis and colleagues,[100] the ET-1-induced reduction of astrocytic gap-junctional communication may in fact not inhibit but contribute to the ET-1-induced generation of SDs. This could provide a possible explanation why ET-1 induces SDs in the neocortex at very low
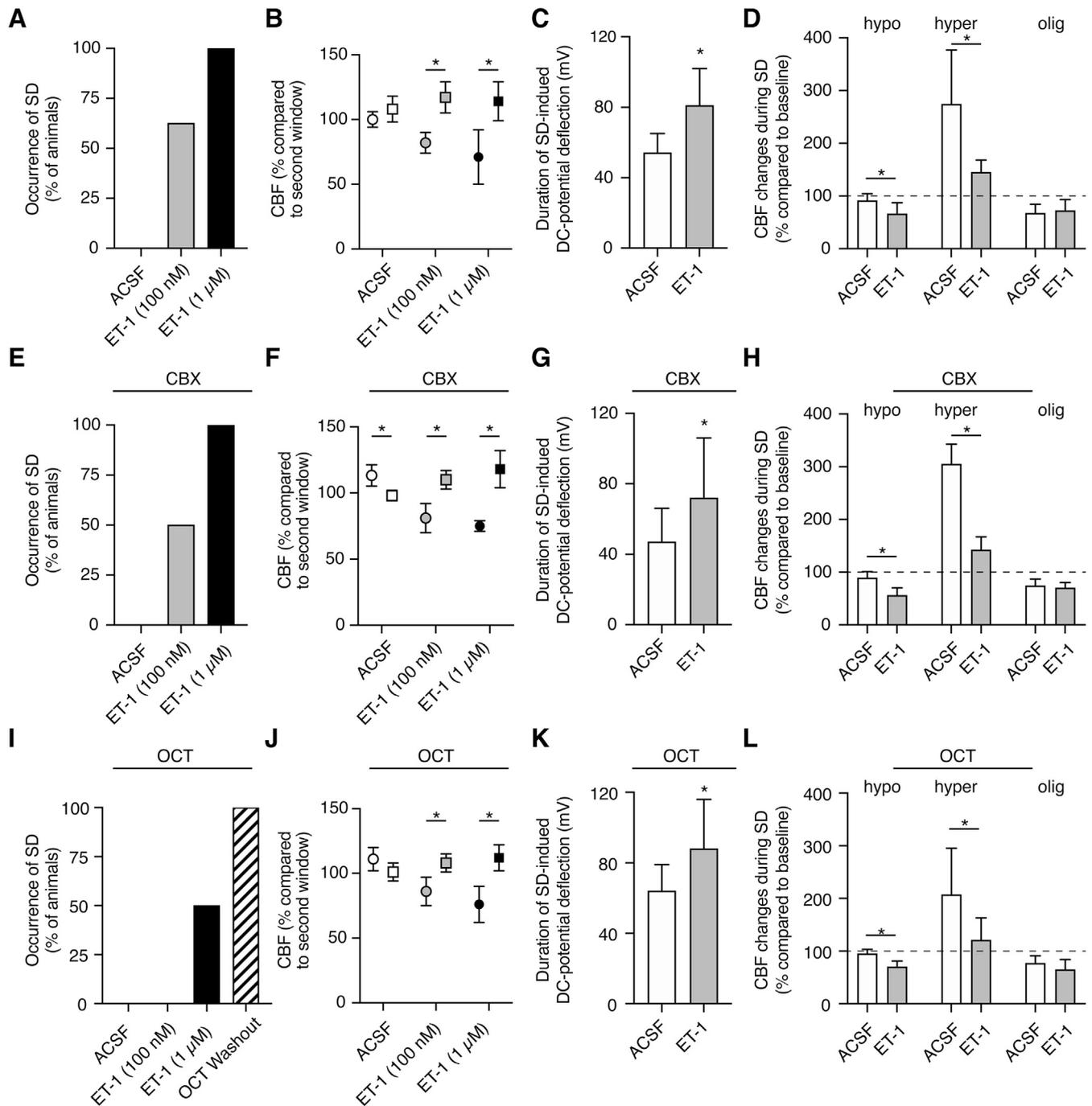
Fig. 2. Effect of carbenoxolone and octanol on the occurrence of ET-1-induced SDs and cerebral blood flow (CBF). (A) Occurrence of SD (% of animals; total, n = 8). (B) CBF gradually and significantly increased in the window perfused with ET-1 (circles) compared to the control window (squares; paired t-test for each comparison). (C) Longer duration of the DC-potential deflection during SD in the ET-1 window (paired t-test). (D) SD-associated hypoemia (hypo) was stronger and hyperemia (hyper) was less pronounced in the ET-1 window, while oligemia (olig) remained similar (paired t-test for each comparison). (E) Carbenoxolone (CBX) had no effect on the occurrence of SDs (% of animals; total, n = 6). (F) Carbenoxolone alone significantly increased CBF (circles denote treatment window) compared to the control window (squares), and the addition of ET-1 led to a gradual significant decrease (paired t-test for each comparison). (G) Longer duration of the DC-potential deflection during SD in the ET-1 window (paired t-test) during carbenoxolone treatment. (H) SD-associated hypoemia was stronger and hyperemia was less pronounced in the ET-1 window, while oligemia remained similar during carbenoxolone treatment (paired t-test for each comparison). (I) Octanol (OCT) shifted the threshold concentration of ET-1 to induce SD to a significantly higher range (p < 0.05, Fisher's Exact Test) (% of animals; total, n = 6). Accordingly, all animals showed SDs in response to ET-1 (1 μM) after washout of octanol. (J) Octanol alone had no significant effect on CBF (circles denote treatment window) compared to the control window (squares), and the addition of ET-1 led to a gradual significant decrease (paired t-test for each comparison). (K) Longer duration of the DC-potential deflection during SD in the ET-1 window (paired t-test) during octanol treatment. (L) SD-associated hypoemia was stronger and hyperemia was less pronounced in the ET-1 window, while oligemia remained similar during octanol treatment (paired t-test for each comparison).

concentrations, although the ET-1-induced decrease of CBF is rather moderate compared to other models of ischemia.[45] On the other hand, in addition to the model of very low brain-topical ET-1 concentrations, there is at least one other pure model of an

ischemic penumbra in which no terminal SD is found that changes into a negative ultraslow potential of high amplitude. This other model is based on air mircoembolisms.[101]

In the present paper, octanol significantly inhibited the occurrence of ET-1-induced SDs *in vivo*. This corresponds well with previous studies on SDs evoked by microinjection or a microdrop of KCl in hippocampal and neocortical slices[71,72] and electrically or mechanically triggered SDs in the isolated chicken retina.[63,73] Because carbenoxolone acts by disrupting connexon particle arrangements,[102] it is a more specific blocker of GJs than octanol, which unspecifically interferes with the membrane lipid bilayer.[103,104] If the effect of octanol on SD would solely be based on its ability to uncouple GJs, we would expect carbenoxolone to be at least equally effective in inhibiting SD. Since this was not the case, effects of octanol not related to the uncoupling of GJs may account for the inhibition of SD.[71] Indeed, octanol also blocks voltage-dependent sodium currents,[105] potentiates GABA$_A$ receptors[106] and inhibits N-methyl-D-aspartate receptors (NMDAR).[106–108] Both the enhancement of GABA$_A$ receptors and in particular the inhibition of NMDARs have been shown to inhibit SDs.[52,109–113] In the previous study of Martins-Ferreira and Ribeiro, it is interesting to note that low concentrations of heptanol and octanol (50–700 μM) in fact increased the velocity of SD in the chicken retina,[73] and that only high concentrations (1 and 10 mM) decreased and finally halted the spread of SD. Given the failure of carbenoxolone to inhibit SD, the findings of Theis and colleagues of an increased SD susceptibility and velocity in mice with genetic reduction of astrocytic gap-junctional communication[100] and the surprisingly high potency of the astrocytic GJ blocker and vasoconstrictor ET-1 to induce SD,[45] we favor the hypothesis that the octanol-induced increase of SD velocity at low concentrations[73] results from blockade of astrocytic GJs, whereas the inhibition of SD at high concentrations may be due to unspecific effects of this long-chain alcohol such as, for example, NMDAR inhibition.[106–108] The concept that octanol inhibits SDs by inhibiting NMDARs would also fit well with the observation that octanol, like other NMDAR antagonists,[110,114–116] progressively loses its SD inhibitory effect with increasing energy depletion.[117] In the present study, octanol (topical application of 2 mM) blocked ET-1-induced SDs in 50% of the rats. For comparison, the NMDAR antagonist MK-801 (intravenous application of 5 mg/kg body weight) previously blocked ET-1-induced SDs in 83% of the rats using the same protocol as in the present study.[45]

A previous experimental study has shown a beneficial effect of octanol on infarct volume after middle cerebral artery occlusion (MCAO) in pentobarbital-anesthetized rats.[64] Octanol reduced infarct volume by 60% and partially inhibited SDs. In principle, similar results have also been previously obtained with other NMDAR antagonists such as MK-801[118,119] or ketamine.[120] Octanol's NMDAR inhibiting action rather than its GJ inhibiting action may thus provide a plausible explanation for its beneficial effect on the infarct volume after MCAO. Another interesting finding was that not only octanol but also carbenoxolone were found to have efficacy in reversing the angiographic arterial spasm after SAH in rabbits.[121] On this basis, the effects of both octanol and carbenoxolone have then been tested in an endovascular perforation model in which SAH was induced under isoflurane anesthesia.[122] Whereas octanol had no effect on neurological deficits induced by SAH and did not reduce neuronal apoptosis, carbenoxolone increased post SAH mortality and strongly exacerbated SAH-induced apoptosis 24 and 72 h after the hemorrhage. Possibly, the different anesthetic protocols could explain at least partially why octanol had no beneficial effect in the SAH model[122] in contrast to the MCAO model.[64] In contrast to pentobarbital, as used

in the MCAO model, isoflurane, as used in the SAH model, significantly inhibits SDs.[123,124] This might be related to its inhibitory effect on NMDARs at the glycine site.[125] Thus, if the beneficial effect of octanol is related to the suppression of SDs by NMDAR inhibition, this should be masked in presence of the NMDAR inhibitor isoflurane. Importantly, the strong exacerbation of the damage by carbenoxolone in the SAH study of Ayer and colleagues[122] makes it further unlikely that the beneficial effect of octanol in the MCAO model resulted from the inhibition of GJs.

5. Conclusions

In summary, our results are consistent with the hypothesis that astrocytic gap-junctional communication does not mediate SD but could rather protect against SD,[100] and that the inhibitory effect of high concentrations of heptanol and octanol on SD is probably unrelated to their effect as GJ inhibitors. The effect of ET-1 as an astrocyte-specific gap-junction inhibitor could contribute to the generation of SDs, although this effect alone is insufficient for SD generation without simultaneous ET-1-induced vasoconstriction.

Declaration of Competing Interest

The authors declare that they have no known competing financial interests or personal relationships that could have appeared to influence the work reported in this paper.

Acknowledgements

References

1. Vergouwen MD, Vermeulen M, van Gijn J, et al. Definition of delayed cerebral ischemia after aneurysmal subarachnoid hemorrhage as an outcome event in clinical trials and observational studies: proposal of a multidisciplinary research group. *Stroke*. 2010;41(10):2391–2395.
2. Vergouwen MD, Etminan N, Ilodigwe D, Macdonald RL. Lower incidence of cerebral infarction correlates with improved functional outcome after aneurysmal subarachnoid hemorrhage. *J Cereb Blood Flow Metab*. 2011;31(7):1545–1553.
3. Neil-Dwyer G, Lang DA, Doshi B, Gerber CJ, Smith PW. Delayed cerebral ischaemia: the pathological substrate. *Acta Neurochir (Wien)*. 1994;131(1–2):137–145.
4. Stoltenburg-Didinger G, Schwarz K. Brain lesions secondary to subarachnoid hemorrhage due to ruptured aneurysms. In: Cervós-Navarro J, Ferszt R, eds. *Stroke and Microcirculation*. Raven Press; 1987:471–480.
5. Birse SH, Tom MI. Incidence of cerebral infarction associated with ruptured intracranial aneurysms. A study of 8 unoperated cases of anterior cerebral aneurysm. Neurology. 1960;10:101–116.
6. Dreier JP, Sakowitz OW, Harder A, et al. Focal laminar cortical MR signal abnormalities after subarachnoid hemorrhage. *Ann Neurol*. 2002;52(6):825–829.
7. Rabinstein AA, Weigand S, Atkinson JL, Wijdicks EF. Patterns of cerebral infarction in aneurysmal subarachnoid hemorrhage. *Stroke*. 2005;36(5):992–997.
8. Schatlo B, Dreier JP, Glasker S, et al. Report of selective cortical infarcts in the primate clot model of vasospasm after subarachnoid hemorrhage. Research Support, N.I.H., Intramural Research Support, Non-U.S. Gov't. Neurosurgery. 2010;67(3):721–8; discussion 728–9.
9. Hossmann KA. Periinfarct depolarizations. *Cerebrovasc Brain Metab Rev. Fall*. 1996;8(3):195–208.
10. Dreier JP, Reiffurth C. Exploitation of the spreading depolarization-induced cytotoxic edema for high-resolution, 3D mapping of its heterogeneous propagation paths. *Proc Natl Acad Sci U S A*. 2017;114(9):2112–2114.
11. Dreier JP. The role of spreading depression, spreading depolarization and spreading ischemia in neurological disease. *Nat Med*. 2011;17(4):439–447.
12. Dreier JP, Lemale CL, Kola V, Friedman A, Schoknecht K. Spreading depolarization is not an epiphenomenon but the principal mechanism of the

cytotoxic edema in various gray matter structures of the brain during stroke. *Neuropharmacology*. 2018;134(Pt B):189–207.

13. Van Harreveld A. Changes in the diameter of apical dendrites during spreading depression. *Am J Physiol*. 1958;192(3):457–463.

14. Nicholson C, Phillips JM, Tobias C, Kraig RP. Extracellular potassium, calcium and volume profiles during spreading depression. In: Syková E, Hñik P, Vyklicky L, eds. *Ion-Selective Microelectrodes and Their Use in Excitable Tissues*. Plenum Press; 1981:211–223.

15. Budde MD, Frank JA. Neurite beading is sufficient to decrease the apparent diffusion coefficient after ischemic stroke. Research Support, N.I.H., Extramural Research Support, N.I.H., Intramural. *Proc Natl Acad Sci U S A*. 2010;107 (32):14472–14477.

16. Takano T, Tian GF, Peng W, et al. Cortical spreading depression causes and coincides with tissue hypoxia. *Nat Neurosci*. 2007;10(6):754–762.

17. Risher WC, Ard D, Yuan J, Kirov SA. Recurrent spontaneous spreading depolarizations facilitate acute dendritic injury in the ischemic penumbra. *J Neurosci*. 2010;30(29):9859–9868.

18. Major S, Huo S, Lemale CL, et al. Direct electrophysiological evidence that spreading depolarization-induced spreading depression is the pathophysiological correlate of the migraine aura and a review of the spreading depolarization continuum of acute neuronal mass injury. *Geroscience*. 2020;42(1):57–80.

19. Dreier JP, Reiffurth C. The Stroke-migraine depolarization continuum. Review. *Neuron*. 2015;86(4):902–922.

20. Hartings JA, Shuttleworth CW, Kirov SA, et al. The continuum of spreading depolarizations in acute cortical lesion development: Examining Leao's legacy. *J Cereb Blood Flow Metab*. 2017;37(5):1571–1594.

21. Dreier JP, Woitzik J, Fabricius M, et al. Delayed ischaemic neurological deficits after subarachnoid haemorrhage are associated with clusters of spreading depolarizations. *Brain.*. 2006;129(Pt 12):3224–3237.

22. Eriksen N, Rostrup E, Fabricius M, et al. Early focal brain injury after subarachnoid hemorrhage correlates with spreading depolarizations. *Neurology*. 2019;92(4):e326–e341.

23. Luckl J, Lemale CL, Kola V, et al. The negative ultraslow potential, electrophysiological correlate of infarction in the human cortex. *Brain*. 2018;141(6):1734–1752.

24. Hartings JA, York J, Carroll CP, et al. Subarachnoid blood acutely induces spreading depolarizations and early cortical infarction. *Brain.*. 2017;140 (10):2673–2690.

25. Dreier JP, Major S, Manning A, et al. Cortical spreading ischaemia is a novel process involved in ischaemic damage in patients with aneurysmal subarachnoid haemorrhage. *Brain.*. 2009;132(Pt 7):1866–1881.

26. Sugimoto K, Nomura S, Shirao S, et al. Cilostazol decreases duration of spreading depolarization and spreading ischemia after aneurysmal subarachnoid hemorrhage. *Ann Neurol*. 2018;84(6):873–885.

27. Bosche B, Graf R, Ernestus RI, et al. Recurrent spreading depolarizations after subarachnoid hemorrhage decreases oxygen availability in human cerebral cortex. *Ann Neurol*. 2010;67(5):607–617.

28. Dohmen C, Sakowitz OW, Fabricius M, et al. Spreading depolarizations occur in human ischemic stroke with high incidence. *Ann Neurol*. 2008;63 (6):720–728.

29. Woitzik J, Hecht N, Pinczolits A, et al. Propagation of cortical spreading depolarization in the human cortex after malignant stroke. Research Support, Non-U.S. Gov't. *Neurology*. 2013;80(12):1095–1102.

30. Pinczolits A, Zdunczyk A, Dengler NF, et al. Standard-sampling microdialysis and spreading depolarizations in patients with malignant hemispheric stroke. *J Cereb Blood Flow Metab*. 2017;37(12):1896–1905.

31. Fabricius M, Fuhr S, Bhatia R, et al. Cortical spreading depression and peri-infarct depolarization in acutely injured human cerebral cortex. *Brain*. 2006;129(Pt 3):778–790.

32. Hartings JA, Bullock MR, Okonkwo DO, et al. Spreading depolarisations and outcome after traumatic brain injury: a prospective observational study. *Lancet Neurol*. 2011;10(12):1058–1064.

33. Helbok R, Schiefecker AJ, Friberg C, et al. Spreading depolarizations in patients with spontaneous intracerebral hemorrhage: Association with perihematomal edema progression. *J Cereb Blood Flow Metab*. 2017;37(5):1871–1882.

34. Beaulieu C, Busch E, de Crespigny A, Moseley ME. Spreading waves of transient and prolonged decreases in water diffusion after subarachnoid hemorrhage in rats. *Magn Reson Med*. 2000;44(1):110–116.

35. Zheng Z, Schoell M, Sanchez-Porras R, Diehl C, Unterberg A, Sakowitz OW. Spreading depolarization during the acute stage of experimental subarachnoid hemorrhage in mice. *Acta Neurochir Suppl*. 2020;127:97–103.

36. Dreier JP, Korner K, Ebert N, et al. Nitric oxide scavenging by hemoglobin or nitric oxide synthase inhibition by N-nitro-L-arginine induces cortical spreading ischemia when K+ is increased in the subarachnoid space. *J Cereb Blood Flow Metab*. 1998;18(9):978–990.

37. Hamming AM, Wermer MJ, Umesh Rudrapatna S, et al. Spreading depolarizations increase delayed brain injury in a rat model of subarachnoid hemorrhage. J Cereb Blood Flow Metab. 2015.

38. Rakers C, Petzold GC. Astrocytic calcium release mediates peri-infarct depolarizations in a rodent stroke model. *J Clin Invest*. 2017;127(2):511–516.

39. Mies G, Iijima T, Hossmann KA. Correlation between peri-infarct DC shifts and ischaemic neuronal damage in rat. *NeuroReport*. 1993;4(6):709–711.

40. Dijkhuizen RM, Beekwilder JP, van der Worp HB, Berkelbach van der Sprenkel KA, Tulleken KA, Nicolay K. Correlation between tissue depolarizations and damage in focal ischemic rat brain. *Brain Res*. 1999;840(1–2):194–205.

41. Rakers C, Schmid M, Petzold GC. TRPV4 channels contribute to calcium transients in astrocytes and neurons during peri-infarct depolarizations in a stroke model. *Glia*. 2017;65(9):1550–1561.

42. Bouley J, Chung DY, Ayata C, Brown Jr RH, Henninger N. Cortical spreading depression denotes concussion injury. *J Neurotrauma*. 2019;36(7):1008–1017.

43. Balança B, Bapteste L, Lieutaud T, et al. Neuronal loss as evidenced by automated quantification of neuronal density following moderate and severe traumatic brain injury in rats. *J Neurosci Res*. 2016;94(1):39–49.

44. Leão AAP. Further observations on the spreading depression of activity in the cerebral cortex. *J Neurophysiol*. 1947;10(6):409–414.

45. Dreier JP, Kleeberg J, Petzold G, et al. Endothelin-1 potently induces Leao's cortical spreading depression in vivo in the rat: a model for an endothelial trigger of migrainous aura?. *Brain*. 2002;125(Pt 1):102–112.

46. Vergouwen MD, Algra A, Rinkel GJ. Endothelin receptor antagonists for aneurysmal subarachnoid hemorrhage: a systematic review and meta-analysis update. Meta-analysis review. Stroke. 2012;43(10):2671–6.

47. Ma J, Huang S, Ma L, Liu Y, Li H, You C. Endothelin-receptor antagonists for aneurysmal subarachnoid hemorrhage: an updated meta-analysis of randomized controlled trials. Crit Care. 2012;16(5):R198.

48. Kleeberg J, Petzold GC, Major S, Dirnagl U, Dreier JP. ET-1 induces cortical spreading depression via activation of the ETA receptor/phospholipase C pathway in vivo. *Am J Physiol Heart Circ Physiol*. 2004;286(4):H1339–H1346.

49. Oliveira-Ferreira AI, Milakara D, Alam M, et al. Experimental and preliminary clinical evidence of an ischemic zone with prolonged negative DC shifts surrounded by a normally perfused tissue belt with persistent electrocorticographic depression. *J Cereb Blood Flow Metab*. 2010;30 (8):1504–1519.

50. Takahashi S, Shibata M, Fukuuchi Y. Role of sodium ion influx in depolarization-induced neuronal cell death by high KCl or veratridine. *Eur J Pharmacol*. 1999;372(3):297–304.

51. Dreier JP, Petzold G, Tille K, et al. Ischaemia triggered by spreading neuronal activation is inhibited by vasodilators in rats. *J Physiol*. 2001;531(Pt 2):515–526.

52. Petzold GC, Windmuller O, Haack S, et al. Increased extracellular K+ concentration reduces the efficacy of N-methyl-D-aspartate receptor antagonists to block spreading depression-like depolarizations and spreading ischemia. *Stroke*. 2005;36(6):1270–1277.

53. Ashton D, Willems R, Wynants J, Van Reempts J, Marrannes R, Clincke G. Altered Na(+)-channel function as an in vitro model of the ischemic penumbra: action of lubeluzole and other neuroprotective drugs. In vitro. *Brain Res*. 1997;745(1–2):210–221.

54. Balestrino M, Young J, Aitken P. Block of (Na+, K+)ATPase with ouabain induces spreading depression-like depolarization in hippocampal slices. *Brain Res*. 1999;838(1–2):37–44.

55. Major S, Petzold GC, Reiffurth C, et al. A role of the sodium pump in spreading ischemia in rats. *J Cereb Blood Flow Metab*. 2017;37(5):1687–1705.

56. Oliveira-Ferreira AI, Major S, Przesdzing I, Kang EJ, Dreier JP. Spreading depolarizations in the rat endothelin-1 model of focal cerebellar ischemia. J Cereb Blood Flow Metab. 2019:271678X19861604.

57. Dreier JP, Kleeberg J, Alam M, et al. Endothelin-1-induced spreading depression in rats is associated with a microarea of selective neuronal necrosis. *Exp Biol Med (Maywood)*. 2007;232(2):204–213.

58. Nedergaard M, Hansen AJ. Spreading depression is not associated with neuronal injury in the normal brain. *Brain Res*. 1988;449(1–2):395–398.

59. Giaume C, Cordier J, Glowinski J. Endothelins inhibit junctional permeability in cultured mouse astrocytes. *Eur J Neurosci*. 1992;4(9):877–881.

60. Blomstrand F, Venance L, Siren AL, et al. Endothelins regulate astrocyte gap junctions in rat hippocampal slices. *Eur J Neurosci*. 2004;19(4):1005–1015.

61. Tence M, Ezan P, Amigou E, Giaume C. Increased interaction of connexin43 with zonula occludens-1 during inhibition of gap junctions by G protein-coupled receptor agonists. *Cell Signal*. 2012;24(1):86–98.

62. Le Bourhis M, Rimbaud S, Grebert D, Congar P, Meunier N. Endothelin uncouples gap junctions in sustentacular cells and olfactory ensheathing cells of the olfactory mucosa. *Eur J Neurosci*. 2014;40(6):2878–2887.

63. Nedergaard M, Cooper AJ, Goldman SA. Gap junctions are required for the propagation of spreading depression. *J Neurobiol*. 1995;28(4):433–444.

64. Rawanduzy A, Hansen A, Hansen TW, Nedergaard M. Effective reduction of infarct volume by gap junction blockade in a rodent model of stroke. *J Neurosurg*. 1997;87(6):916–920.

65. Kunkler PE, Kraig RP. Calcium waves precede electrophysiological changes of spreading depression in hippocampal organ cultures. Research Support, Non-U. S. Gov't., P.H.S. J Neurosci. May 1 1998;18(9):3416-25.

66. Nedergaard M. Direct signaling from astrocytes to neurons in cultures of mammalian brain cells. *Science*. 1994;263(5154):1768–1771.

67. Somjen GG. Mechanisms of spreading depression and hypoxic spreading depression-like depolarization. *Physiol Rev*. 2001;81(3):1065–1096.

68. Chuquet J, Hollender L, Nimchinsky EA. High-resolution in vivo imaging of the neurovascular unit during spreading depression. Comparative Study Research Support, U.S. Gov't, Non-P.H.S. *J Neurosci.* 2007;27(15):4036–4044.

69. Enger R, Tang W, Vindedal GF, et al. Dynamics of Ionic Shifts in Cortical Spreading Depression. *Cereb Cortex.* Nov 2015;25(11):4469–4476.

70. Peters O, Schipke CG, Hashimoto Y, Kettenmann H. Different mechanisms promote astrocyte Ca2+ waves and spreading depression in the mouse neocortex. *J Neurosci.* 2003;23(30):9888–9896.

71. Vilagi I, Klapka N, Luhmann HJ. Optical recording of spreading depression in rat neocortical slices. *Brain Res.* 2001;898(2):288–296.

72. Largo C, Tombaugh GC, Aitken PG, Herreras O, Somjen GG. Heptanol but not fluoroacetate prevents the propagation of spreading depression in rat hippocampal slices. *J Neurophysiol.* 1997;77(1):9–16.

73. Martins-Ferreira H, Ribeiro LJ. Biphasic effects of gap junctional uncoupling agents on the propagation of retinal spreading depression. In Vitro Research Support, Non-U.S. Gov't. Braz J Med Biol Res. 1995;28(9):991-4.

74. Windmuller O, Lindauer U, Foddis M, et al. Ion changes in spreading ischaemia induce rat middle cerebral artery constriction in the absence of NO. *Brain.* 2005;128(Pt 9):2042–2051.

75. Kang EJ, Major S, Jorks D, et al. Blood-brain barrier opening to large molecules does not imply blood-brain barrier opening to small ions. Research Support, Non-U.S. Gov't. Neurobiol Dis. 2013;52:204-18.

76. Bostanci MO, Bagirici F. Anticonvulsive effects of carbenoxolone on penicillin-induced epileptiform activity: an in vivo study. *Neuropharmacology.* 2007;52(2):362–367.

77. Gigout S, Louvel J, Kawasaki H, et al. Effects of gap junction blockers on human neocortical synchronization. *Neurobiol Dis.* 2006;22(3):496–508.

78. Gajda Z, Szupera Z, Blazso G, Szente M. Quinine, a blocker of neuronal cx36 channels, suppresses seizure activity in rat neocortex in vivo. *Epilepsia..* 2005;46(10):1581–1591.

79. Herreras O, Largo C, Ibarz JM, Somjen GG, Martin del Rio R. Role of neuronal synchronizing mechanisms in the propagation of spreading depression in the in vivo hippocampus. J Neurosci. 1994;14(11 Pt 2):7087-98.

80. Shapiro BE. Osmotic forces and gap junctions in spreading depression: a computational model. *J Comput Neurosci.* 2001;10(1):99–120.

81. Sutor B, Hagerty T. Involvement of gap junctions in the development of the neocortex. Research Support, Non-U.S. Gov'tReview. *Biochim Biophys Acta, Rev Biomembr.* 2005;1719(1–2):59–68.

82. Sutor B, Luhmann HJ. Development of excitatory and inhibitory postsynaptic potentials in the rat neocortex. Research Support, Non-U.S. Gov't Review. *Perspect Dev Neurobiol.* 1995;2(4):409–419.

83. Woodruff AR, McGarry LM, Vogels TP, Inan M, Anderson SA, Yuste R. State-dependent function of neocortical chandelier cells. In Vitro Research Support, N.I.H., Extramural Research Support, Non-U.S. Gov't. *J Neurosci.* 2011;31(49):17872–17886.

84. Cruikshank SJ, Landisman CE, Mancilla JG, Connors BW. Connexon connexions in the thalamocortical system. Research Support, N.I.H., Extramural Research Support, Non-U.S. Gov't Review. *Prog Brain Res.* 2005;149:41–57.

85. Fukuda T, Kosaka T, Singer W, Galuske RA. Gap junctions among dendrites of cortical GABAergic neurons establish a dense and widespread intercolumnar network. Research Support, Non-U.S. Gov't. *J Neurosci.* 2006;26(13):3434–3443.

86. Schade JP. Maturational aspects of EEG and of spreading depression in rabbit. *J Neurophysiol.* 1959;22(3):245–257.

87. Dzhala V, Ben-Ari Y, Khazipov R. Seizures accelerate anoxia-induced neuronal death in the neonatal rat hippocampus. *Ann Neurol.* 2000;48(4):632–640.

88. Bures J. The ontogenetic development of steady potential differences in the cerebral cortex in animals. *Electroencephalogr Clin Neurophysiol.* 1957;9(1):121–130.

89. Hablitz JJ, Heinemann U. Alterations in the microenvironment during spreading depression associated with epileptiform activity in the immature neocortex. *Brain Res Dev Brain Res.* 1989;46(2):243–252.

90. Maslarova A, Alam M, Reiffurth C, Lapilover E, Gorji A, Dreier JP. Chronically epileptic human and rat neocortex display a similar resistance against spreading depolarization in vitro. *Stroke.* 2011;42(10):2917–2922.

91. Menyhart A, Zolei-Szenasi D, Puskas T, et al. Spreading depolarization remarkably exacerbates ischemia-induced tissue acidosis in the young and aged rat brain. Sci Rep. 2017;7(1):1154.

92. Traub RD, Whittington MA, Gutierrez R, Draguhn A. Electrical coupling between hippocampal neurons: contrasting roles of principal cell gap junctions and interneuron gap junctions. *Cell Tissue Res.* 2018;373(3):671–691.

93. Juszczak GR, Swiergiel AH. Properties of gap junction blockers and their behavioural, cognitive and electrophysiological effects: animal and human studies. *Prog Neuro-Psychopharmacol Biol Psychiatry.* 2009;33(2):181–198.

94. Schmitz D, Schuchmann S, Fisahn A, et al. Axo-axonal coupling. a novel mechanism for ultrafast neuronal communication. *Neuron.* 2001;31(5):831–840.

95. Beraneck M, Uno A, Vassias I, et al. Evidence against a role of gap junctions in vestibular compensation. *Neurosci Lett.* 2009;450(2):97–101.

96. Chaytor AT, Marsh WL, Hutcheson IR, Griffith TM. Comparison of glycyrrhetinic acid isoforms and carbenoxolone as inhibitors of EDHF-type relaxations mediated via gap junctions. *Endothelium.* 2000;7(4):265–278.

97. Nielsen AN, Fabricius M, Lauritzen M. Scanning laser-Doppler flowmetry of rat cerebral circulation during cortical spreading depression. *J Vasc Res.* 2000;37(6):513–522.

98. Desroches M, Faugeras O, Krupa M, Mantegazza M. Modeling cortical spreading depression induced by the hyperactivity of interneurons. J Comput Neurosci. 2019.

99. Jansen NA, Dehghani A, Linssen MML, Breukel C, Tolner EA, van den Maagdenberg A. First FHM3 mouse model shows spontaneous cortical spreading depolarizations. *Ann Clin Transl Neurol.* 2020;7(1):132–138.

100. Theis M, Jauch R, Zhuo L, et al. Accelerated hippocampal spreading depression and enhanced locomotory activity in mice with astrocyte-directed inactivation of connexin43. Research Support, Non-U.S. Gov't. *J Neurosci.* 2003;23(3):766–776.

101. Nozari A, Dilekoz E, Sukhotinsky I, et al. Microemboli may link spreading depression, migraine aura, and patent foramen ovale. *Ann Neurol.* 2010;67(2):221–229.

102. Goldberg GS, Moreno AP, Bechberger JF, et al. Evidence that disruption of connexon particle arrangements in gap junction plaques is associated with inhibition of gap junctional communication by a glycyrrhetinic acid derivative. *Exp Cell Res.* 1996;222(1):48–53.

103. Rozental R, Srinivas M, Spray DC. How to close a gap junction channel. Efficacies and potencies of uncoupling agents. *Methods Mol Biol.* 2001;154:447–476.

104. Weingart R, Bukauskas FF. Long-chain n-alkanols and arachidonic acid interfere with the Vm-sensitive gating mechanism of gap junction channels. *Pflugers Arch.* 1998;435(2):310–319.

105. Nelson WL, Makielski JC. Block of sodium current by heptanol in voltage-clamped canine cardiac Purkinje cells. *Circ Res.* 1991;68(4):977–983.

106. Dildy-Mayfield JE, Mihic SJ, Liu Y, Deitrich RA, Harris RA. Actions of long chain alcohols on GABAA and glutamate receptors: relation to in vivo effects. *Br J Pharmacol.* 1996;118(2):378–384.

107. McLarnon JG, Wong JH, Sawyer D, Baimbridge KG. The actions of intermediate and long-chain n-alkanols on unitary NMDA currents in hippocampal neurons. *Can J Physiol Pharmacol.* 1991;69(10):1422–1427.

108. Ogata J, Shiraishi M, Namba T, Smothers CT, Woodward JJ, Harris RA. Effects of anesthetics on mutant N-methyl-D-aspartate receptors expressed in Xenopus oocytes. *J Pharmacol Exp Ther.* 2006;318(1):434–443.

109. Marrannes R, Willems R, De Prins E, Wauquier A. Evidence for a role of the N-methyl-D-aspartate (NMDA) receptor in cortical spreading depression in the rat. *Brain Res.* 1988;457(2):226–240.

110. Lauritzen M, Hansen AJ. The effect of glutamate receptor blockade on anoxic depolarization and cortical spreading depression. *J Cereb Blood Flow Metab.* 1992;12(2):223–229.

111. Wang M, Li Y, Lin Y. GABAA receptor alpha2 subtype activation suppresses retinal spreading depression. *Neuroscience.* 2015;298:137–144.

112. Unekawa M, Tomita Y, Toriumi H, Suzuki N. Suppressive effect of chronic peroral topiramate on potassium-induced cortical spreading depression in rats. *Cephalalgia.* 2012;32(7):518–527.

113. Köhling R, Koch UR, Hagemann G, Redecker C, Straub H, Speckmann EJ. Differential sensitivity to induction of spreading depression by partial disinhibition in chronically epileptic human and rat as compared to native rat neocortical tissue. *Brain Res.* 2003;975(1–2):129–134.

114. Hernandez-Caceres J, Macias-Gonzalez R, Brozek G, Bures J. Systemic ketamine blocks cortical spreading depression but does not delay the onset of terminal anoxic depolarization in rats. *Brain Res.* 1987;437(2):360–364.

115. Muller M, Somjen GG. Inhibition of major cationic inward currents prevents spreading depression-like hypoxic depolarization in rat hippocampal tissue slices. *Brain Res.* 1998;812(1–2):1–13.

116. Madry C, Haglerod C, Attwell D. The role of pannexin hemichannels in the anoxic depolarization of hippocampal pyramidal cells. *Brain..* Dec 2010;133(Pt 12):3755–3763.

117. Aitken PG, Tombaugh GC, Turner DA, Somjen GG. Similar propagation of SD and hypoxic SD-like depolarization in rat hippocampus recorded optically and electrically. *J Neurophysiol.* 1998;80(3):1514–1521.

118. Dirnagl U, Tanabe J, Pulsinelli W. Pre- and post-treatment with MK-801 but not pretreatment alone reduces neocortical damage after focal cerebral ischemia in the rat. *Brain Res.* 1990;527(1):62–68.

119. Iijima T, Mies G, Hossmann KA. Repeated negative DC deflections in rat cortex following middle cerebral artery occlusion are abolished by MK-801: effect on volume of ischemic injury. *J Cereb Blood Flow Metab.* 1992;12(5):727–733.

120. Schoknecht K, Kikhia M, Lemale CL, et al. The role of spreading depolarizations and electrographic seizures in early injury progression of the rat photothrombosis stroke model. J Cereb Blood Flow Metab. 2020:271678X20915801.

121. Hong T, Wang H, Wang Y, Wang H. Effects of gap junctional blockers on cerebral vasospasm after subarachnoid hemorrhage in rabbits. *Neurol Res.* 2009;31(3):238–244.

122. Ayer R, Chen W, Sugawara T, Suzuki H, Zhang JH. Role of gap junctions in early brain injury following subarachnoid hemorrhage. *Brain Res.* 2010;1315:150–158.

123. Takagaki M, Feuerstein D, Kumagai T, Gramer M, Yoshimine T, Graf R. Isoflurane suppresses cortical spreading depolarizations compared to

propofol–implications for sedation of neurocritical care patients. *Exp Neurol.* 2014;252:12–17.

124. Kudo C, Toyama M, Boku A, et al. Anesthetic effects on susceptibility to cortical spreading depression. *Neuropharmacology.* 2013;67:32–36.

125. Dickinson R, Peterson BK, Banks P, et al. Competitive inhibition at the glycine site of the N-methyl-D-aspartate receptor by the anesthetics xenon and isoflurane: evidence from molecular modeling and electrophysiology. *Anesthesiology.* 2007;107(5):756–767.